

# The Electronic States of $U^{4+}$ in $U(PO_4)Cl$ : An Example for Angular Overlap Modeling of $5f^n$ Systems

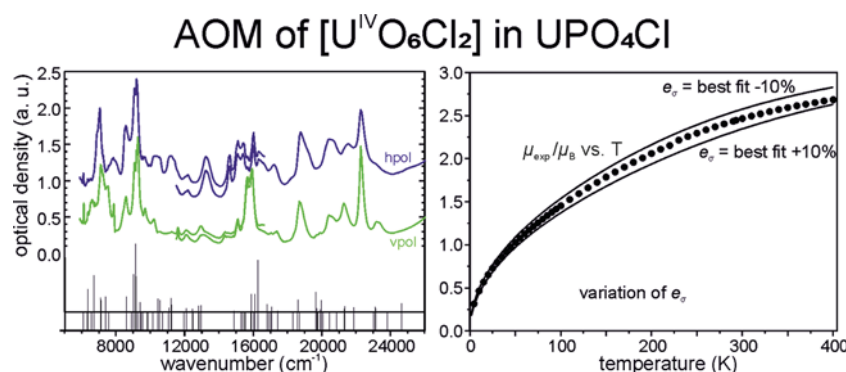
Anna Bronova,<sup>†</sup> Thomas Bredow,<sup>‡</sup> Robert Glaum,<sup>\*,†</sup> and Werner Urland<sup>§</sup>

<sup>†</sup>Institute of Inorganic Chemistry, Rheinische Friedrich-Wilhelms-Universität, Gerhard-Domagk-Straße 1, D-53121 Bonn, Germany

<sup>‡</sup>Mulliken Center for Theoretical Chemistry, Rheinische Friedrich-Wilhelms-Universität, Beringstr. 4, D-53121 Bonn, Germany

<sup>§</sup>Chemistry Department, University of Fribourg, Chemin du Musée 9, CH-1700 Fribourg, Switzerland

## Supporting Information



**ABSTRACT:** Detailed experimental data on  $UPO_4Cl$  comprising single-crystal UV/vis/NIR spectra and temperature-dependent magnetic susceptibilities form the basis for the investigation of the electronic structure of the  $U^{4+}$  cation in  $UPO_4Cl$ . For modeling of the observed physical properties the *angular overlap model* (AOM) was successfully employed. The computations were performed using the newly developed computer program BonnMag. The calculations show that all electronic transitions and the magnetic susceptibility as well as its temperature dependence are well-reproduced within the AOM framework. Using Judd–Ofelt theory BonnMag allows estimation of the relative absorption coefficients of the electronic transitions with reasonable accuracy. Ligand field splitting for states originating from f-electron configurations are determined. Slater–Condon–Shortley parameters and the spin–orbit coupling constant for  $U^{4+}$  were taken from literature. The good transferability of AOM parameters for  $U^{4+}$  is confirmed by calculations of the absorption spectra of  $UP_2O_7$  and  $(U_2O)(PO_4)_2$ . The effect of variation of the fit parameters is investigated. AOM parameters for  $U^{4+}$  ( $5f$ ) are compared to those of the rare-earth elements ( $4f$ ) and transition metals ( $3d$ ).

## INTRODUCTION

Calculation of the energies of f-electron configurations and of physical properties based thereon within the framework of the *angular overlap model* (AOM)<sup>1–4</sup> are of interest due to the various technically important properties of  $f^n$  systems. These properties include magnetic ( $\chi$ ,  $g$ ) and optical behavior. For their investigation, fast and reliable calculations with a computationally efficient approach are desirable for screening purpose and for analyses of the electronic structure of rare earth metal compounds. Up to now, only  $f^1–f^3$  and  $f^{11}–f^{13}$  systems could be treated within the AOM (implemented in the programs SURGEV,<sup>5</sup> AOMX,<sup>6</sup> and LIGFIELD<sup>7</sup>). For  $4f^n$  systems featuring large spin–orbit coupling and small ligand field effects the assignment of the split terms using the well-known Dieke diagrams<sup>8</sup> is straightforward, ignoring, however, ligand field splitting. Since in  $5f^n$  systems ligand field splitting and spin–orbit coupling effects are of similar magnitude, such a simple analysis of the optical spectra is impossible. For a reasonable assignment of the observed electronic transitions

and estimation of their absorption coefficients, symmetry analysis of the underlying electronic states is required as prerequisite for the application of Judd–Ofelt theory.<sup>9,10</sup> In this study, we present examples of such calculations using the newly developed computer program BonnMag.<sup>11</sup> As basis for our detailed treatment of metal–ligand interactions and of the ligand field influence highly resolved, polarized single-crystal absorption spectra and temperature-dependent magnetic susceptibilities of  $UPO_4Cl$  shown in the preceding paper of this issue are used.<sup>12</sup>

Our AOM calculations using BonnMag allow separation of the effects of ligand field splitting and spin–orbit coupling on the energy of the observed electronic states. Because of the simple and fast procedure, a large number of calculations with variation of parameters is possible. Thus, assessment of the “best fit AOM parameters” is accomplished. We want to

emphasize here that as further advantages the AOM approach has no symmetry restrictions and that the parameters are well-founded in molecular orbital theory.<sup>1–4</sup> It will be shown that the computer program BonnMag<sup>11</sup> is well-suited for performing these calculations. On request BonnMag may be obtained from the authors (A.B. and R.G).

## ■ THE ANGULAR OVERLAP APPROACH

In AOM<sup>1–4</sup> the global ligand field, which can be given by 10 Dq or  $\Delta$  for transition metals, is split into the contributions of individual bonding interactions ( $\sigma$ ,  $\pi$ ,  $\delta$ ) between the ligand and metal orbitals (d or f). Chromophores with different (low-symmetry) geometric structure can be described without symmetry restriction by this model using transferable and chemically meaningful bonding parameters. Note: In a strict sense, these parameters describe for most ligands the antibonding effect between metal and ligand orbitals. The ligand field is described by the sum of all  $\sigma$  and  $\pi$  interactions between the ligands and the central metal atom. The  $\delta$  interaction is included in AOM theory but is neglected in most studies due to its small contribution.<sup>13</sup> The interaction parameters are denoted as  $e_\sigma$  and  $e_\pi$  (cm<sup>-1</sup>). For these parameters transferability from already parametrized compounds is assumed (and confirmed for many cases) when considering new systems. Thus, the AOM has some predictive power. Interpretation of ligand behavior is possible due to the correlation of the bonding parameters with the metal–ligand interaction. It is important to note that AOM contains a number of approximations. Those are the use of Slater–Condon–Shortley (SCS) theory for the description of the electronic states of the free ion and restriction of the individual ligand–metal interaction to one  $\sigma$ - and two perpendicular  $\pi$ -bonds. A fundamental aspect of this model is the parametrization of the metal–ligand interactions by fitting of the calculated properties to experimental data. Thus, AOM accounts in a simple way for the ligand field influence. Already, during the 1960s and 1970s the AOM was used for calculations of properties of rare earth metal compounds that are based on the energies of their f electronic states.<sup>4,14,15</sup> These investigations were limited to systems  $f^1$ – $f^3$ ,  $f^{11}$ – $f^{13}$ , and, in most cases, to high-symmetry coordination polyhedra. The main reason for these limitations was the lack of computing power.

For d<sup>n</sup> systems several computer programs are widely spread in the scientific community, CAMMAG by GERLOCH<sup>16</sup> (PC Version by RILEY<sup>17</sup>), AOMX by SCHMIDTKE, ATANASOV, and ADAMSKY,<sup>6</sup> and LIGFIELD by BENDIX.<sup>7</sup> With these programs the energies of all electronic states and, depending on these energies, magnetic susceptibilities (as well as g values) for d<sup>n</sup> systems can be calculated.

## ■ ANGULAR OVERLAP MODEL WITH BONNMAG

For the calculation of absorption spectra and magnetic susceptibilities of UPO<sub>4</sub>Cl (f<sup>2</sup>) the computer program BonnMag<sup>11</sup> was used. This program is based on SURGEV, which was developed by W. Urland during the 1970s.<sup>5</sup> Its code bears also some resemblance to CAMMAG.<sup>16,17</sup> As its predecessor, BonnMag uses the angular overlap approach to approximate the ligand field effect. All possible configuration interactions are considered by the *coefficients of fractional parentage* (CFP) and *reduced matrix elements* (RME).<sup>18,19</sup> These have been implemented in the program. In contrast to its predecessors, BonnMag allows calculation of energies of f–f

transitions, magnetic susceptibilities, crystal susceptibilities, and g-tensors (for odd numbers of f-electrons) for the complete range of f<sup>n</sup> systems. An additional improvement of BonnMag is the calculation of (relative) absorption coefficients<sup>9,10</sup> for each transition and a symmetry analysis of the split terms with assignment of their irreducible representations.

**Parametrization.** BonnMag includes several atomic and interatomic parameters. The SCS parameters  $F_2$ ,  $F_4$ , and  $F_6$ <sup>20</sup> and the spin–orbit coupling constant  $\zeta$  are needed for the calculation of the transition energies of the free ion. The AOM parameters  $e_\sigma$  and  $e_\pi$  describe the various metal–ligand interactions. To account for different metal–ligand distances  $e_\sigma$  and  $e_\pi$  are assumed to depend on  $d(M-L)^{-n}$ .

As prerequisite for the calculations a global coordinate system must be defined that allows the geometric description of the ML<sub>m</sub> chromophore (see Figure 1). For the calculation of

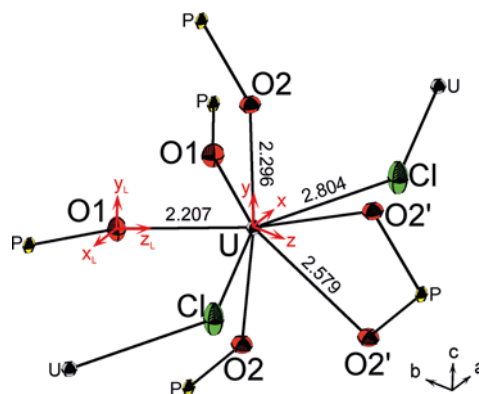


**Figure 1.** ORTEP representation of the [U<sup>IV</sup>O<sub>6</sub>Cl<sub>2</sub>] chromophore in UPO<sub>4</sub>Cl given with the second coordination sphere and coordinate systems for the central atom (global coordinate system) and one ligand as example (index L).<sup>12</sup>

orientation dependent properties, a careful choice of this global coordinate system is required. For details on this topic, we refer to ref 16. The calculated transition energies are, however, independent of the chosen coordinate system. The global coordinate system must be defined according to the point-group symmetry to get the irreducible representations of the eigenstates. In addition, the local ligand coordinate systems must be set for each ligand in the chromophore. Here the atoms of the first and, if necessary, the second coordination sphere are used. “Dummy” atoms can be introduced too, to allow facile definition of directions. The second coordination sphere can be used for definition of the ligand coordinate systems if an anisotropic  $\pi$ -interaction must be accounted for in the calculations.

As already mentioned Judd–Ofelt Theory<sup>9,10</sup> is applied for estimating the absorption coefficients for electronic transitions in f<sup>n</sup> systems. It contains several approximations. In general electric dipole transitions are allowed, if  $\Delta S = 0$ ,  $\Delta L = 0$  or  $\pm 1$ , and  $\Delta J = 0$  or  $\pm 1$  ( $J = 0 \leftrightarrow J = 0$  forbidden) and Laporte’s rule is obeyed.<sup>21</sup> Judd–Ofelt theory is based on the assumption that configuration interaction between  $4f^n$  and high-energy  $4f^{n-1}5d^1$  states lends intensity to the otherwise Laporte forbidden transitions between pure  $4f^n$  states. Configuration interaction depends on the symmetry of the interacting states; thus, symmetry analysis is required. Judd–Ofelt theory further assumes an average energy for excited  $4f^{n-1}5d^1$  configuration above the states derived from the  $4f^n$  configuration.

For simplification of the calculations Judd–Ofelt parameters  $\Omega_n$  ( $n = 2, 4, 6$ ) are treated as empirical parameters and determined by fitting to experimental line strengths. Note that Judd–Ofelt theory does not allow calculation of absolute absorption coefficients.

A detailed account of the code of BonnMag and of the implemented routines will be given elsewhere.

## ■ AOM PARAMETRIZATION FOR THE $[\text{U}^{\text{IV}}\text{O}_6\text{Cl}_2]$ CHROMOPHORE

In  $\text{UPO}_4\text{Cl}$  uranium (Wyckoff position 4c, site symmetry  $C_{2v}$ ) is coordinated by six oxygen and two chlorine atoms (see Figure 1). There are four different distances  $d(\text{M}-\text{L})$  with  $d(\text{U}-\text{O}1) = 2.207 \text{ \AA}$ ,  $d(\text{U}-\text{O}2) = 2.296 \text{ \AA}$ ,  $d(\text{U}-\text{O}2') = 2.579 \text{ \AA}$ , and  $d(\text{U}-\text{Cl}) = 2.804 \text{ \AA}$ .<sup>22</sup>

The SCS parameters  $F_2$ ,  $F_4$ , and  $F_6$  and the spin–orbit coupling constant  $\zeta$  for the  $\text{U}^{4+}$  ion were taken from the analysis of the UV/vis spectrum of the  $[\text{U}^{\text{IV}}\text{Cl}_6]$  chromophore in  $\text{Cs}_2\text{U}^{\text{IV}}\text{Cl}_6$ .<sup>23</sup> These values were obtained in the reference by a fit of the calculated transition energies to the experimental data. The AOM parameters  $e_\sigma(\text{U}-\text{O})$  and  $e_{\pi,\text{iso}}(\text{U}-\text{O})$ , for a given distance  $d(\text{U}-\text{O})$ , were obtained by matching the calculated magnetic susceptibilities and excited-state energies against the observed data. The  $e_{\pi,\text{iso}}$  were taken as one-quarter of the corresponding  $e_\sigma$ . The parameters  $e_\sigma(\text{U}-\text{Cl}) = 1270 \text{ cm}^{-1}$  and  $e_{\pi,\text{iso}}(\text{U}-\text{Cl}) = 318 \text{ cm}^{-1}$  were transferred from  $\text{Cs}_2\text{U}^{\text{IV}}\text{Cl}_6$ .<sup>31</sup> The different distances  $d(\text{U}-\text{Cl})$  in  $\text{UPO}_4\text{Cl}$  and  $\text{Cs}_2\text{UCl}_6$  were accounted for by relation 1. “Best fit” parameters (Table 1) were derived by visual comparison of calculated and

**Table 1. Best-Fit Parameters<sup>a</sup> for the Angular Overlap Modeling of the  $[\text{U}^{\text{IV}}\text{O}_6\text{Cl}_2]$  Chromophore in  $\text{UPO}_4\text{Cl}$**

Slater–Condon–Shortley parameters ( $\text{cm}^{-1}$ )				
$F_2 = 190.9$	$F_4 = 33.74$	$F_6 = 3.99675$	$(\beta = F_2/F_{2,\text{f.i.}} = 0.82)$	
Slater–Condon–Shortley parameters of the free $\text{U}^{4+}$ ion ( $\text{cm}^{-1}$ ) <sup>27</sup>				
$F_{2,\text{f.i.}} = 234.73$	$F_{4,\text{f.i.}} = 41.35$	$F_{6,\text{f.i.}} = 4.10$		
spin–orbit coupling constant ( $\text{cm}^{-1}$ )				
$\zeta = 1797.02$				
Stevens-orbital reduction factor <sup>28</sup>				
$k = 0.95$				
interaction parameters $e_m(\text{U}-\text{O})$ and $e_m(\text{U}-\text{Cl})$ ( $m: \sigma, \pi$ )				
ligand	distance ( $\text{\AA}$ )	$e_\sigma$ ( $\text{cm}^{-1}$ )	$e_{\pi,\text{iso}}$ ( $\text{cm}^{-1}$ )	$e_\pi/e_\sigma$
O1	2.207	2052	513	0.25
O2	2.296	1556	389	0.25
O2'	2.579	690	173	0.25
Cl	2.804	1270	318	0.25
Judd–Ofelt parameters ( $1 \times 10^{-24} \text{ m}^2$ )				
$\Omega_2 = 1.078$	$\Omega_4 = 2.014$	$\Omega_6 = 0.4529$		

<sup>a</sup>From visual comparison of observed and calculated transition energies, line strengths, and the dependence of magnetic moment on temperature.

observed data. This procedure leads to  $e_\sigma(\text{U}-\text{O}) = 2052 \text{ cm}^{-1}$  and  $e_{\pi,\text{iso}}(\text{U}-\text{O}) = 513 \text{ cm}^{-1}$  for  $d(\text{U}-\text{O})_{\text{min}} = 2.207 \text{ \AA}$ . To account for the different interatomic distances  $d(\text{U}-\text{O})$  in  $\text{UPO}_4\text{Cl}$ ,  $e_\sigma(d)$  and  $e_{\pi,\text{iso}}(d)$  are scaled in the following way.<sup>24</sup>

$$e_m(d) = e_m(d(\text{U}-\text{L})_{\text{min}}) \cdot \left( \frac{d(\text{U}-\text{L})_{\text{min}}}{d(\text{U}-\text{L})} \right)^7 \quad (m: \sigma, \pi; \text{L: O, Cl}) \quad (1)$$

Second-sphere ligand effects<sup>25</sup> were neglected in our modeling, to keep the parametrization as simple as possible. With the same reasoning, only isotropic  $\pi$ -interactions were considered.

For the AOM calculations on the chromophores  $[\text{U}^{\text{IV}}\text{O}_6]$  (octahedral with slight angular distortion in  $\text{UP}_2\text{O}_7$ ) and  $[\text{U}^{\text{IV}}\text{O}_7]$  in  $\text{U}_2\text{O}(\text{PO}_4)_2$  (see Figure 6) the parameters were directly transferred from  $\text{UPO}_4\text{Cl}$  (same  $F_2$ ,  $F_4$ ,  $F_6$ , and  $\zeta$ ;  $e_\sigma$  adjusted to distance  $\text{U}-\text{O}$ ). Details on these chromophores and the AOM parameters are given in Figures S1 and S2 and in Tables S3 to S7.

For the calculation of absorption coefficients (line strength) the well-established Judd–Ofelt parameters  $\Omega_n$  ( $n = 2, 4, 6$ ) of  $\text{Pr}^{3+}$  ( $f^2$ )<sup>26</sup> were taken as initial values. The good fit between calculated and observed line strengths for the  $\text{U}^{4+}$  ion in  $\text{UPO}_4\text{Cl}$  (Figure 2) and further uranium(IV) phosphates

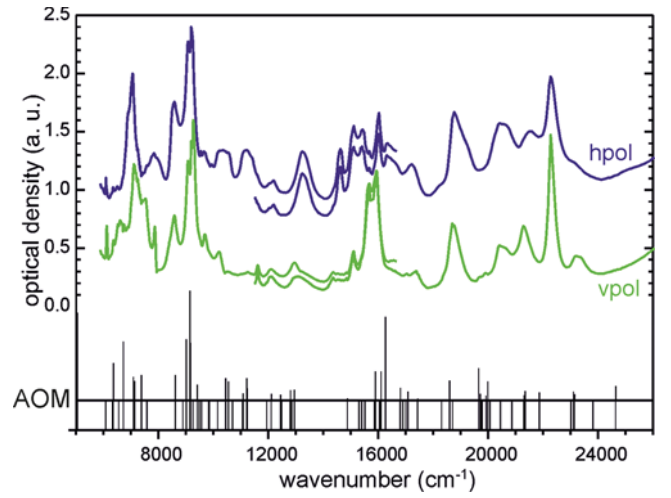


**Figure 2.** Polarized electronic absorption spectra of a (010) crystal face of  $\text{U}(\text{PO}_4)\text{Cl}$ . “hpol” and “vpol” denote perpendicular polarization directions of the incident light beam. Angular overlap results (zero-phonon lines) (AOM) with estimated intensities (Judd–Ofelt theory).

(Figure 6) was eventually obtained by reducing the third parameter  $\Omega_6$  from  $4.529 \times 10^{-24} \text{ m}^2$  to  $0.4529 \times 10^{-24} \text{ m}^2$ . Table 1 gives a summary of all parameters.

## ■ RESULTS AND DISCUSSION

**Summary of the Experimental Data.** Figure 2 shows the good match between observed and calculated electronic transition energies (zero-phonon lines). It also shows good agreement between observed and calculated line strengths. This confirms that electronic states of  $\text{U}^{4+}$  can be described well by using SCS parameters and the AOM parameters  $e_\sigma$  and  $e_\pi$  given in Table 1. Because of the good compliance between observed spectra and the results from modeling, a safe assignment of the observed electronic transitions is achieved (Figure 2; see also Table S1). Deviations between observed and calculated electronic transition energies are generally small ( $<500 \text{ cm}^{-1}$ ). It appears that the generally good match between observed and calculated absorption coefficients is less good at higher wavenumbers, above  $20000 \text{ cm}^{-1}$ . Effective Bohr magneton numbers<sup>29</sup>  $\mu_{\text{eff}}$  calculated using the same parameters show a very good match with the experimental data (Figure 7b).

**Variation of Parameters.** To check the dependence of the theoretical results on the parameters the SCS parameter  $F_2$  was varied, and the calculated optical transition energies were

compared to those from the best-fit calculation. The ratios  $F_2/F_4$  and  $F_2/F_6$  were kept constant in these calculations. Varying  $F_2$  by  $\pm 5\%$  leads to a shift (up to  $\sim 1500\text{ cm}^{-1}$ ) of the calculated transition energies to lower and higher values, respectively (see Figure 3). The good match between calculated and

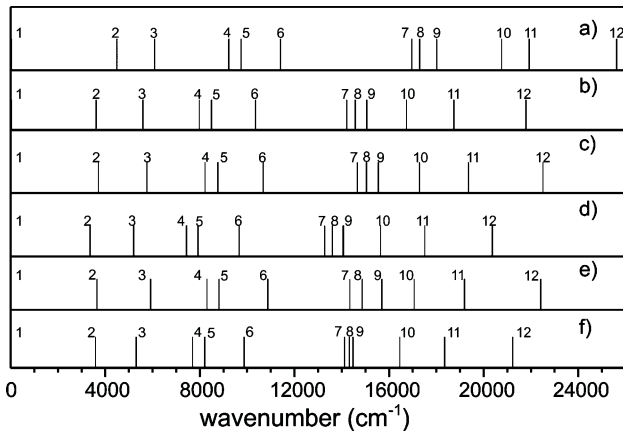


**Figure 3.** Transition energies for the free ion  $U^{4+}$  ( $e_\sigma = e_\pi = 0\text{ cm}^{-1}$ ) calculated with different sets  $F_2$ ,  $F_4$ ,  $F_6$ , and  $\zeta$ . Condon–Shortley parameters and spin–orbit coupling for the free  $U^{4+}$  ion derived from arc spectra,  $\zeta_{\text{free ion}} = 1969\text{ cm}^{-1}$  (a), best-fit SCS parameters for  $U^{4+}$  used in present AO modeling {derived for the chromophore  $[U^{IV}Cl_6]$ ,  $\zeta = 1797.02\text{ cm}^{-122}$  (b)}, best-fit parameters increased by 5% ( $F_2$  and  $\zeta$ ) (c), best-fit parameters decreased by 5% ( $F_2$  and  $\zeta$ ) (d), best-fit SCS parameters with  $\zeta = 1886.87\text{ cm}^{-1}$ , (e), best-fit SCS parameters with  $\zeta = 1707.17\text{ cm}^{-1}$  (f). Sequence of the free ion states 1 to 12:  ${}^3H_4$ ,  ${}^3F_2$ ,  ${}^3H_5$ ,  ${}^3F_3$ ,  ${}^3F_4$ ,  ${}^3H_6$ ,  ${}^3P_0$ ,  ${}^1D_2$ ,  ${}^1G_4$ ,  ${}^3P_1$ ,  ${}^1I_6$ ,  ${}^3P_2$ .

experimental energies is lost. As expected the calculated effective Bohr magneton number  $\mu_{\text{eff}}$  does not show a significant dependence on  $F_2$  (Figure 7g,i).

The SCS parameters available in literature for the free  $U^{4+}$  ion (see Table 1) were determined from the measured emission spectrum of gas-phase  $U^{4+}$  for the high-energy region of  $43\,000\text{--}165\,000\text{ cm}^{-1}$ . The energies calculated in our investigation with best-fit SCS parameters are at much lower wave numbers (see Figure 3). Nevertheless, the nephelauxetic ratio ( $\beta = F_2/F_{2,\text{fi}} = 0.82$ ) is, as expected, considerably smaller than values for  $\beta$  observed for lanthanide ions.

By variation of the interaction parameters  $e_\sigma$  and  $e_\pi$  and therefore of the strength of the ligand field the effect of these parameters on the energies of the optical transitions was investigated. The results of a series of calculations with  $e_\sigma$  ranging from zero to 120% of the best-fit values are summarized in Figure 4 ( $e_\pi = 1/4 e_\sigma$ ). By increasing of the interaction parameters (ligand field strength), the splitting of the parental terms increases as expected. By this gradual increase of the ligand field assignment of the resulting terms to the parental terms becomes possible. Inspection of the splitting and the  $J$  projections of the split terms as a function of  $e_\sigma$  shows also that term interaction becomes increasingly important with increasing  $e_\sigma$ . Thus, only for adjacent states at low  $e_\sigma$  the inspection of their  $J$  projection leads to a safe assignment of the resulting terms to their parental terms. Above 110% of the best-fit values for the  $e_\sigma$  the relation to the parental term is completely lost due to the increasing term interaction.

For the excited-state energies calculated with the best-fit parameters (Table 1), an unambiguous assignment to certain parental terms is impossible without additional criteria. It

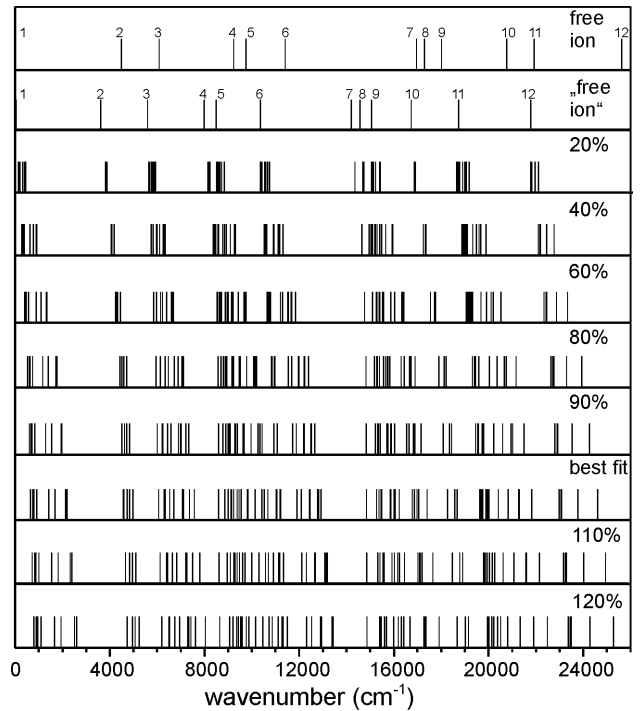


**Figure 4.** Calculated transitions for the free ion  $U^{4+}$  (“free ion” means that the nephelauxetic ratio  $\beta$  was considered) and the chromophore  $[UO_6Cl_2]$  with increasing strength of the ligand field (different interaction parameters  $e_\sigma$  and  $e_\pi$ ). The percentages refer to the best-fit  $e_\sigma$  and  $e_\pi$  values from Table 1. Sequence of the free ion states 1 to 12:  ${}^3H_4$ ,  ${}^3F_2$ ,  ${}^3H_5$ ,  ${}^3F_3$ ,  ${}^3F_4$ ,  ${}^3H_6$ ,  ${}^3P_0$ ,  ${}^1D_2$ ,  ${}^1G_4$ ,  ${}^3P_1$ ,  ${}^1I_6$ ,  ${}^3P_2$ .  $\zeta_{\text{free ion}} = 1969\text{ cm}^{-1}$ ,  $\zeta_{\text{AOM}} = 1797.02\text{ cm}^{-1}$ .

becomes obvious from Figure 4 that only for  $e_\sigma$  in the range from 90% to 110% of the best-fit values a reasonable match between observed and calculated transition energies is achieved. As shown in Figure 7 the temperature dependence of the effective Bohr magneton number  $\mu_{\text{eff}}$  is far more susceptible to variation of  $e_\sigma$ . These comparisons allow an estimate of the accuracy of the best-fit parameter set. Further corroboration for the magnitude of  $e_\sigma$  is obtained by comparison of the observed and calculated splitting of the parental states (Figure 5). The influence of the scaling of the interaction parameters with distance  $e_\sigma \approx d(U-O)^{-x}$  ( $x = 5.0, 7.0, 8.0$ ) is shown in Figure 5. The various exponents lead in all calculations to rather good matches with the observed transition energies and the effective number of Bohr magnetons. Yet, these data are not very sensitive to  $x$ , which in turn cannot be determined more precisely.

BonnMag calculates the  $J$  projections and determines the irreducible representation for each eigenstate by procedures described in literature.<sup>36–38</sup> From the  $J$  projections and the symmetry analysis of the eigenvector the parental term with the highest contribution to a given eigenstate is determined. As example, Figure 5 shows the contribution of various parental terms to the states between  $8000$  and  $11\,000\text{ cm}^{-1}$ . With this analysis the influence of the magnitude of  $e_\sigma$  (ligand field) on the splitting can be better understood.

The calculations of  $J$  projections confirm that term interaction between neighboring terms is significant for  $U^{4+}$ . Above  $10\,000\text{ cm}^{-1}$   ${}^3F_4$  interacts with the neighboring state  ${}^3H_6$ , so that  ${}^3H_6$  has a considerable admixture of the lower state. Because of the symmetry analysis and calculation of absorption

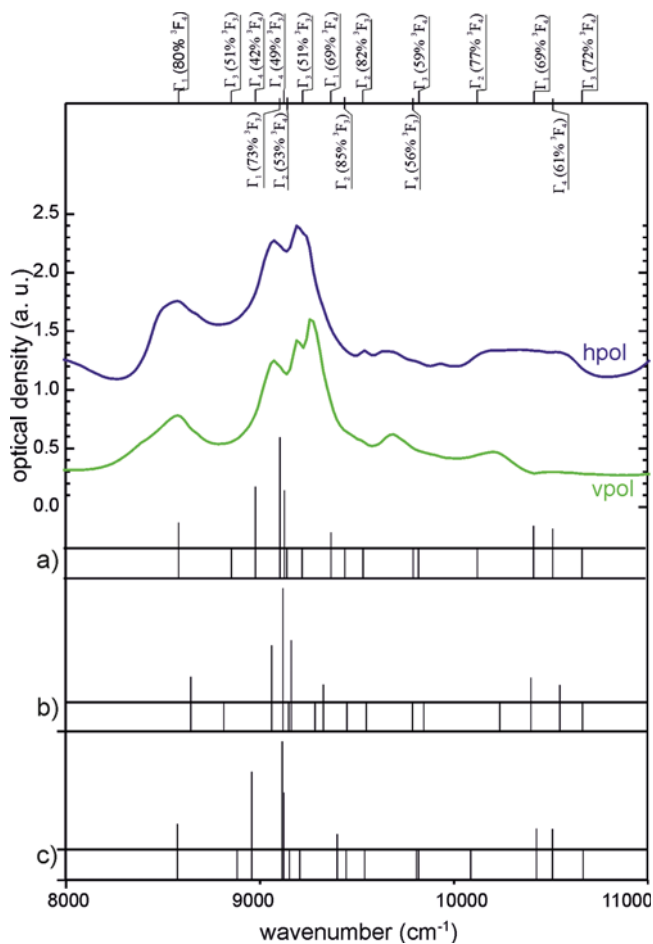


**Figure 5.** UV/vis/NIR-spectra of  $\text{UPO}_4\text{Cl}$  with the transition energies for the region between 8000 and 11 000  $\text{cm}^{-1}$  calculated by BonnMag and symmetry analysis of the terms. Angular overlap modeling (zero-phonon lines) with estimated intensities (according to Judd–Ofelt theory) with scaling factor  $e_\sigma \approx d(\text{U-O})^{-7}$  (a),  $e_\sigma \approx d(\text{U-O})^{-5}$  (b),  $e_\sigma \approx d(\text{U-O})^{-8}$  (c). The parental terms with the largest contribution to the split term are given in parentheses.

coefficients, the quantitative assignment of the terms to the observed transitions becomes possible.

For the 8000–11 000  $\text{cm}^{-1}$  region (see Figure 5) of the spectra the irreducible representations of the split terms were determined. The point group  $C_{2v}$  of the chromophore  $[\text{U}^{\text{IV}}\text{O}_6\text{Cl}_2]$  was used. We show that according to Judd–Ofelt theory some transitions have no intensity (Figures 2 and 5). The ground state has an irreducible representation  $\Gamma_1 (A_1)$ . Therefore, not all transitions are allowed by an electric dipole mechanism.<sup>21</sup> Transitions from the ground state into  $\Gamma_1 (A_1)$  or  $\Gamma_4 (B_2)$  are dipole-allowed, whereby the intensities of the transitions into  $\Gamma_2 (B_1)$  or  $\Gamma_3 (A_2)$  are zero.<sup>21</sup>

Absorption energies and line strengths for  $\text{UP}_2\text{O}_7$ <sup>30</sup> and  $(\text{U}_2\text{O})(\text{PO}_4)_2$ <sup>22</sup> were calculated with parameter sets matching the parametrization of  $\text{UPO}_4\text{Cl}$  (see Figure 6 and Supporting Information Figures S1 and S2 and Tables S3 and S4). These results are in fair agreement with the observed absorption spectra.

The last parameters that were varied are the spin–orbit coupling constant  $\zeta$  and Stevens–orbital reduction factor  $k$ . The spin–orbit coupling constant taken from literature leads to the best fit between calculated and observed magnetic susceptibilities. To improve the agreement between the calculated and the

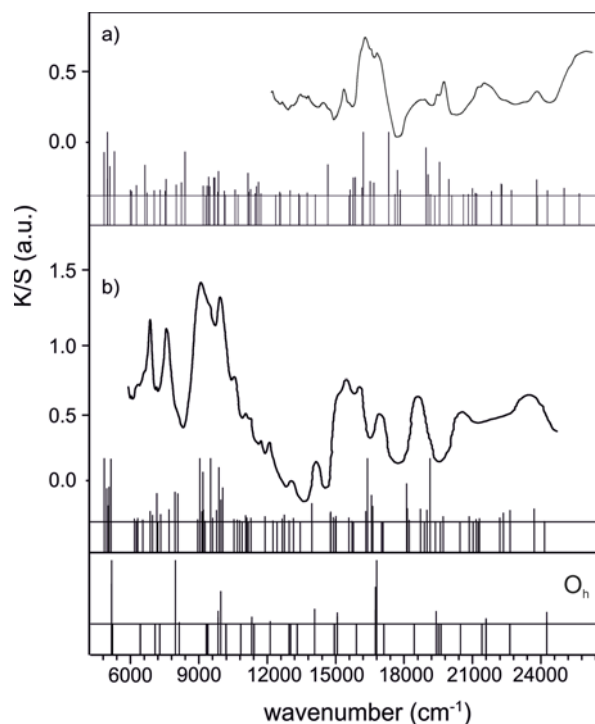


**Figure 6.** Powder reflectance spectra of  $(\text{U}_2\text{O})(\text{PO}_4)_2$ <sup>22</sup> (a) and  $\text{UP}_2\text{O}_7$ <sup>30</sup> (b). Angular overlap modeling (zero-phonon lines) with estimated relative intensities (according to Judd–Ofelt theory) for the real symmetry and ideal octahedron.

experimental magnetic data the Stevens–orbital reduction factor<sup>28</sup>  $k$  was reduced to 95%. For a consistency check of the used parameter set several calculations of the effective Bohr magneton number  $\mu_{\text{eff}}$  as a function of the temperature with two values for  $k$  were performed. In Figure 7a–c comparison between results obtained with  $k = 1.0$ ,  $k = 0.95$ , and  $k = 0.9$  is shown. For  $k = 1.0$  (see Figure 7a) the calculated moments are larger; for  $k = 0.9$  they are smaller than the measured ones.

As already mentioned the best fit for the absorption coefficients was obtained by reducing the third Judd–Ofelt parameter  $\Omega_6$  from  $4.529 \times 10^{-24} \text{ m}^2$  (for  $\text{Pr}^{3+}$ <sup>26</sup>) to  $0.4529 \times 10^{-24} \text{ m}^2$  for the  $\text{U}^{4+}$  ion. Parameters  $\Omega_2 = 1.078 \times 10^{-24} \text{ m}^2$  and  $\Omega_4 = 2.014 \times 10^{-24} \text{ m}^2$  (also from  $\text{Pr}^{3+}$ ) were kept unchanged. Only by decreasing parameter  $\Omega_6$  with respect to the literature, value for  $\text{Pr}^{3+}$  a good fit of the calculated to the experimental line strength was achieved. Variation of  $\Omega_2$  or  $\Omega_4$  does not change the relative line strengths of the absorption coefficients and has only a scaling effect. Only variation of  $\Omega_6$  allowed adjusting of the relative magnitudes of the line strengths (“absorption coefficients”). Our calculations show that many of the calculated transitions have no intensity within Judd–Ofelt theory. Thus, the intensity criterion is essential for the assignment of the observed transitions.

The variation procedures show that these parameters cannot be arbitrarily selected or changed. Because of the combination of absorption spectra and magnetic measurement a reliable parameter set is found.

**Discussion of Obtained AOM Parameters.** For  $\text{Cs}_2\text{UCl}_6$  (chromophore  $[\text{U}^{\text{IV}}\text{Cl}_6]$ ) with  $d(\text{U-Cl}) = 2.621 \text{ \AA}$ <sup>31</sup> the interaction parameters  $e_\sigma(\text{U-Cl}) = 1489 \text{ cm}^{-1}$  and  $e_{\pi,\text{iso}}(\text{U-Cl}) = 338 \text{ cm}^{-1}$ <sup>32</sup> have been reported. Using BonnMag with these parameters the energy levels for the chromophore  $[\text{U}^{\text{IV}}\text{Cl}_6]$  were calculated and compared to those observed and calculated

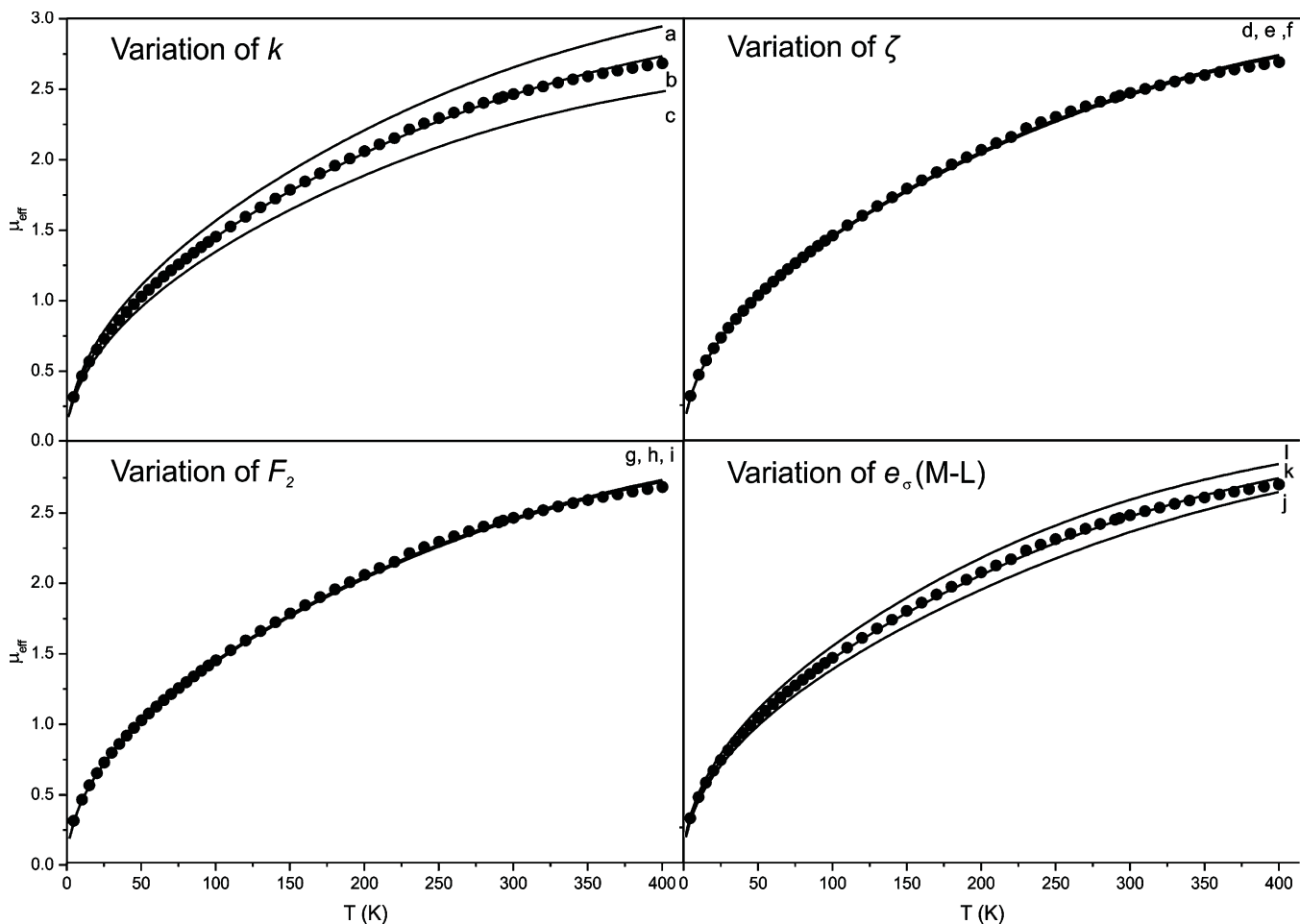


**Figure 7.** Graphical representation of the measured effective Bohr magneton number  $\mu_{\text{eff}}$  (arb units) vs  $T$  (K) for  $\text{UPO}_4\text{Cl}$  and comparison to the calculated  $\mu_{\text{eff}}$  (solid lines). (a)  $k = 1.0$ , (b)  $k = 0.95$  (best fit), (c)  $k = 0.90$ , (d)  $\zeta =$  best fit +5%, (e) best fit, (f)  $\zeta =$  best fit -5%, (g)  $F_2 =$  best-fit values +5%, (h) best fit, (i)  $F_2 =$  best-fit values -5%, (j)  $e_\sigma =$  best-fit values +10%, (k) best fit, (l)  $e_\sigma =$  best-fit values -10%.

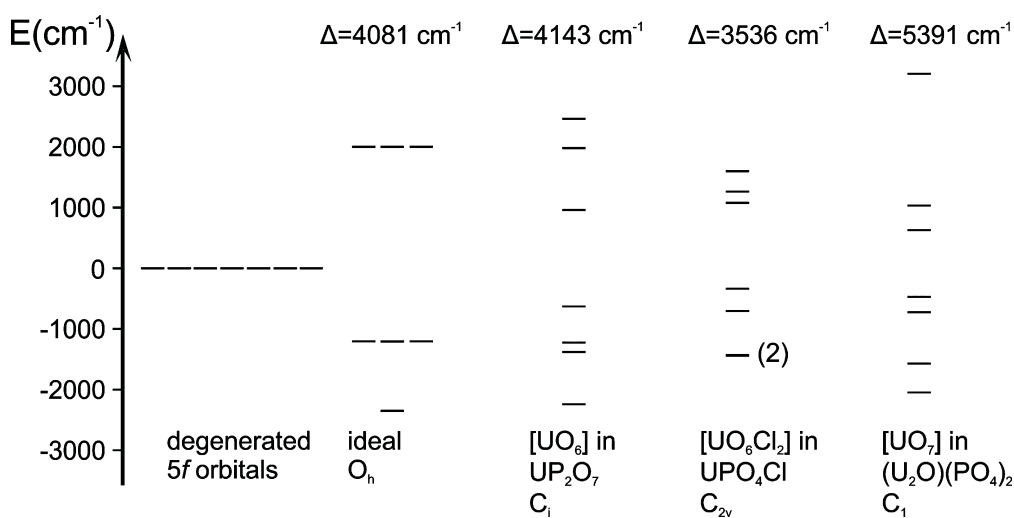


**Figure 8.** Splitting of the  $f$ -orbitals by the chromophores  $[\text{U}^{\text{IV}}\text{O}_6]$  ( $O_h$  symmetry),  $[\text{U}^{\text{IV}}\text{O}_6]$  in  $\text{UP}_2\text{O}_7$ ,  $[\text{U}^{\text{IV}}\text{O}_6\text{Cl}_2]$  in  $\text{UPO}_4\text{Cl}$ , and  $[\text{U}^{\text{IV}}\text{O}_7]$  in  $\text{U}_2\text{O}(\text{PO}_4)_2$  (energies to scale) compared to the ligand field splittings according to Wybourne.

by SATTEN<sup>23</sup> (see Table S2). The two sets of calculated energies fit perfectly, thus demonstrating the compliance of the two calculations.

For  $\text{UO}_2$  (chromophore  $[\text{U}^{\text{IV}}\text{O}_8]$ ) with an uranium–oxygen distance  $d(\text{U}-\text{O}) = 2.3729 \text{ \AA}$  the parameter  $e_\sigma(\text{U}-\text{O}) = 1908$

$\text{cm}^{-1}$  was obtained by GAJEK and MULAK.<sup>33</sup> In case of  $\text{U}^{4+}$  doped in  $\text{ThSiO}_4$   $e_\sigma(\text{U}-\text{O})_{2.417 \text{ \AA}} = 1650 \text{ cm}^{-1}$  has been reported.<sup>33</sup> In contrast, the values for  $e_\sigma(\text{U}-\text{O})$  obtained for  $\text{UPO}_4\text{Cl}$  in this work are  $\sim 30\%$  smaller for comparable distances. Reasons for this difference are not yet clear.

Calculations with variation of the ratio  $e_\pi/e_\sigma = 0.15, 0.25,$  and  $0.35$  showed no significant influence of the assumed magnitude of the  $\pi$ -interaction on the magnetic moment per  $U^{4+}$  and the excited-state energies. An accurate characterization of the ground-state splitting by ligand field effects, for example, by resonance Raman spectroscopy,<sup>34</sup> might allow or even require a more detailed description of the  $\pi$ -interaction, though.

The AOM parameters of  $U^{4+}$  in  $UPO_4Cl$  are  $\sim 5$  times larger than the typical values for  $Pr^{3+}$  and significantly smaller than those for 3d transition metals.

**Extraction of Ligand Field Splitting from the Angular Overlap Model Calculation.** The splitting of the f-orbitals caused by the various ligand fields is calculated from the AOM parameters  $e_\sigma$  and  $e_\pi$  of the  $[U^{IV}O_6Cl_2]$  chromophore and their effect on an  $f^1$  system (Figure 8). For these calculations, the SCS parameters as well as the spin-orbit coupling constant were set to zero. Because of the low symmetry ( $C_{2v}$ ) of the  $[U^{IV}O_6Cl_2]$  chromophore in  $UPO_4Cl$  the degeneracy of the seven f-orbitals is lifted completely. In the same way the splitting of the f-orbitals by an ideally octahedral  $[U^{IV}O_6]$  chromophore, the  $[U^{IV}O_6]$  chromophore with slight angular distortion in  $UP_2O_7$  and the  $[U^{IV}O_7]$  chromophore in  $(U_2O)(PO_4)_2$  were calculated (Figure 8). The influence of the small angular distortions ( $89.5^\circ \leq \angle(O,U,O) \leq 90.5^\circ$ ; see Figure S1) and their effect on the  $[U^{IV}O_6]$  chromophore in  $UP_2O_7$  is quite remarkable and leads to the complete removal of the orbital degeneracy compared to the ideal octahedron (see Figure 8).

By using the definition of the ligand field strength given by Wybourne<sup>35</sup> (eq 2)  $\Delta$  for  $UPO_4Cl$ ,  $UP_2O_7$  (real and ideal geometries), and  $(U_2O)(PO_4)_2$  was calculated:  $\Delta(UPO_4Cl) = 3536 \text{ cm}^{-1}$ ,  $\Delta(UO_6, \text{ideal}) = 4081 \text{ cm}^{-1}$ ,  $\Delta(UP_2O_7, \text{real}) = 4143 \text{ cm}^{-1}$ ,  $\Delta((U_2O)(PO_4)_2) = 5391 \text{ cm}^{-1}$ . The Wybourne parameters used for these calculations were obtained from the AOM parameters in BonnMag. The smallest  $\Delta$  is observed for  $UPO_4Cl$ . As expected these ligand field splittings are smaller than those typically found for 3d metal complexes ( $\Delta \approx 10\,000 \text{ cm}^{-1}$ ) but larger than those of chromophores containing rare earth element ( $\Delta \approx 1000 \text{ cm}^{-1}$ ).

$$S = \left[ \frac{1}{3} \sum_k \frac{1}{2k+1} ((B_0^k)^2 + 2 \sum_{q>0} ((\text{Re}B_q^k)^2 + (\text{Im}B_q^k)^2)) \right]^{1/2} \quad (2)$$

## CONCLUSIONS

The presented AOM calculations provide a good match to the observed magnetic susceptibilities, transition energies, and (relative) absorption coefficients of the  $[U^{IV}O_6Cl_2]$  chromophore in  $UPO_4Cl$ . These calculations also demonstrate the versatility and power of the new computer program BonnMag. The significance of the AOM parameters obtained for  $UPO_4Cl$  has been assessed by variation of each parameter within chemically reasonable limits. Matching the results of AOM simultaneously against observed absorption spectra and magnetic susceptibilities puts rather narrow limits to the parameter space. It is shown that thus-obtained AOM parameters for  $UPO_4Cl$  can be transferred to  $UP_2O_7$  and  $(U_2O)(PO_4)_2$ . Compared to literature data derived for  $UO_2$  the value obtained here for  $e_\sigma(U-O)_{\text{norm.}}$  is  $\sim 30\%$  smaller.

## ASSOCIATED CONTENT

### Supporting Information

The Supporting Information is available free of charge

Tabulated data for  $UPO_4Cl$ : calculated and observed transition energies, line strengths (I) with assignment of the parental terms for the region between 0 and  $26\,000 \text{ cm}^{-1}$  (measured transition are above  $6000 \text{ cm}^{-1}$ ). Irreducible representations are given for split terms of the ground state and for the range  $8000\text{--}11\,000 \text{ cm}^{-1}$ . Tabulated calculated and observed transition energies for the chromophore  $[U^{IV}Cl_6]$  in  $Cs_2ZrCl_6$ . Tabulated AOM (BonnMag) input file for the chromophore  $[U^{IV}O_6]$  in  $UP_2O_7$  (real geometry). Tabulated AOM (BonnMag) input file for the chromophore  $[U^{IV}O_6]$  (ideal octahedron). Tabulated AOM parameters for the chromophore  $[U^{IV}O_6]$  (ideal octahedron) and distorted geometry in  $UP_2O_7$ . Tabulated AOM (BonnMag) input file for  $U_2O(PO_4)_2$  ( $[U^{IV}O_7]$  chromophore). Tabulated AOM parameters for the  $[U^{IV}O_7]$  chromophore in  $U_2O(PO_4)_2$ . ORTEP representation of the  $[U^{IV}O_6]$  chromophore in  $UP_2O_7$  given with coordinate systems for the central atom (global coordinate system) and one ligand as example (index L). ORTEP representation of the  $[U^{IV}O_7]$  chromophore in  $U_2O(PO_4)_2$  given with coordinate systems for the central atom (global coordinate system) and one ligand as example (index L). (PDF)

## AUTHOR INFORMATION

### Corresponding Author

\*E-mail: [rglaum@uni-bonn.de](mailto:rglaum@uni-bonn.de).

### Author Contributions

The manuscript was written through contributions of all authors. All authors have given approval to the final version of the manuscript.

### Notes

The authors declare no competing financial interest.

## ACKNOWLEDGMENTS

The authors want to express their sincerest thanks to the reviewers, who pointed out shortcomings of the original manuscript and suggested improvements in great detail.

## REFERENCES

- Jørgensen, C. K.; Pappalardo, R.; Schmidtke, H.-H. *J. Chem. Phys.* **1963**, *39*, 1422.
- Richardson, D. E. *J. Chem. Educ.* **1993**, *70*, 372.
- Larsen, E.; LaMar, G. N. *J. Chem. Educ.* **1974**, *51*, 633.
- Urland, W. *Chem. Phys.* **1976**, *14*, 393.
- Urland, W. Habilitation thesis, University of Gießen, 1980.
- (a) Atanasov, M.; Schmidtke, H.-H. *Chem. Phys.* **1988**, *124*, 205. (b) Adamsky, H. *Computer program AOMX*; University of Düsseldorf, 1996. <http://www.aomx.de/docs/html/aomxeh.html>.
- (a) Bendix, J.; Brorson, M.; Schäffer, E. *Inorg. Chem.* **1993**, *32*, 2838. (b) Bendix, J. "Ligfield": An Extensive Program Package for Ligand-Field Calculations on a Personal Computer, *29th International Conference on Coordination Chemistry*, Lausanne, Switzerland, 1992.
- Dieke, G. H. *Spectra and energy levels of rare earth ions in crystals*; Interscience Publishers: New York, 1968.
- Judd, B. R. *Phys. Rev.* **1962**, *127*, 750.
- Ofelt, G. S. *J. Chem. Phys.* **1962**, *37*, 511.

- (11) Bronova, A. *planned Ph.D. thesis*, University of Bonn, 2016.
- (12) Bronova, A.; Droß, T.; Glaum, R.; Lueken, H.; Speldrich, M.; Urland, W. *Inorg. Chem.* **2016**, in preparation. DOI: [10.1021/acs.inorgchem.6b00438](https://doi.org/10.1021/acs.inorgchem.6b00438).
- (13) Schaeffer, C. E. *Struct. Bonding (Berlin)*; Springer: NY, 1968; Vol. 5.
- (14) Urland, W. *Chem. Phys. Lett.* **1977**, *46*, 457.
- (15) Urland, W. *Chem. Phys. Lett.* **1977**, *50*, 445.
- (16) (a) Gerloch, M. *Magnetism and Ligand Field Theory*; Cambridge Univ. Press, 1983. (b) Gerloch, M.; McMeeking, R. F. *J. Chem. Soc., Dalton Trans.* **1975**, 2443.
- (17) Riley, M. *Inorg. Chim. Acta* **1998**, *268*, 55.
- (18) Racah, G. *Phys. Rev.* **1943**, *63*, 367.
- (19) Nielson, C. W.; Koster, G. F. *Spectroscopic Coefficients for  $p^n$ ,  $d^n$  and  $f^n$  Configurations*; Cambridge MIT Press, 1963.
- (20) Condon, E. U.; Shortley, G. H. *The Theory of Atomic Spectra*; Cambridge Univ. Press, 1967.
- (21) Hüfner, S. *Optical Spectra of Transparent Rare Earth Compounds*; Academic Press: New York, 1978.
- (22) Dross, T. Ph.D. Thesis, University of Bonn, 2004. urn:nbn:de:hbz:5N-03770.
- (23) Satten, R. A.; Schreiber, C. L.; Wong, E. Y. *J. Chem. Phys.* **1965**, *42*, 162.
- (24) Urland, W. *Chem. Phys.* **1979**, *38*, 407.
- (25) Reinen, D.; Atanasov, M.; Lee, S.-L. *Coord. Chem. Rev.* **1998**, *175*, 91.
- (26) (a) Leavitt, R. P.; Morrison, C. A. *J. Chem. Phys.* **1980**, *73*, 749. (b) Weber, M. J. *Phys. Rev.* **1967**, *157*, 262. (c) Weber, M. J. *Optical Properties of Ions in Crystals*; Wiley Interscience: New York, 1967.
- (27) Wyart, J. F.; Kaufman, V.; Sugar, J. *Phys. Scr.* **1980**, *22*, 389.
- (28) Stevens, K. W. H. *Proc. R. Soc.* **1954**, *A219*, 542.
- (29) Hatscher, S. T.; Lueken, H.; Schilder, H.; Urland, W. *Pure Appl. Chem.* **2005**, *77*, 497.
- (30) Cabeza, A.; et al. *J. Solid State Chem.* **1996**, *121*, 181.
- (31) Schleid, T.; Meyer, G.; Morss, L. R. *J. Less-Common Met.* **1987**, *132*, 69.
- (32) Warren, K. D. *Inorg. Chem.* **1977**, *16*, 2008.
- (33) (a) Gajek, Z.; Mulak, J. *J. Phys.: Condens. Matter* **1992**, *4*, 427. (b) Gajek, Z. *J. Magn. Magn. Mater.* **2004**, *272-276*, E415. (c) Gajek, Z. *J. Magn. Magn. Mater.* **1988**, *76*, 363.
- (34) Skoog, D. A.; Holler, J.; Crouch, S. R. *Principles of Instrumental Analysis*; Brooks/Cole: Boston, 2006.
- (35) Goerller-Walrand, C.; Binnemans, K. In *Handbook on the Physics and Chemistry of Rare Earths*; Gschneidner, K. A., Eyring, L., Eds.; Elsevier: Amsterdam, 1996; Vol. 23.
- (36) Zare, R. N. *Angular Momentum*; Wiley & Sons: New York, 1988.
- (37) Bethe, H. *Ann. Phys.* **1929**, *395*, 133.
- (38) Cotton, F. A. *Chemical Applications of Group Theory*; Wiley & Sons: New York, 1990.